Study on Aqueous Mixtures of Fullerene-Based Star Ionomers and Sodium Dodecyl Sulfate Using Small Angle Scattering with Contrast Variation

ARTICLE *in* THE JOURNAL OF PHYSICAL CHEMISTRY A · NOVEMBER 2002

Impact Factor: 2.69 · DOI: 10.1021/jp020346r

7 AUTHORS, INCLUDING:

H. Frielinghaus
Forschungszentrum Jülich
137 PUBLICATIONS **1,418** CITATIONS

Study on Aqueous Mixtures of Fullerene-Based Star Ionomers and Sodium Dodecyl Sulfate Using Small Angle Scattering with Contrast Variation

U. Jeng,[†] T.-L. Lin,*[,†] Y. Hu,[†] T.-S. Chang,[†] T. Canteenwala,[‡] L. Y. Chiang,[‡] and H. Frielinghaus[§]

Department of Engineering and System Science, National Tsing Hua University, Hsinchu 30043, Taiwan, Center for Condensed Matter Sciences, National Taiwan University, Taipei 10617, Taiwan, and Institut für Festkörperforschung Forschungszentrum, Jülich GmbH D-52425, Jülich, Germany

Received: February 6, 2002; In Final Form: October 22, 2002

Using small angle neutron scattering (SANS) and small angle X-ray scattering (SAXS), we have studied aqueous mixtures of fullerene-based ionomers, $C_{60}[(CH_2)_4SO_3Na]_6$ (FC_4S), and sodium dodecyl sulfate (SDS). With the contrast variation provided by SAXS and a selected deuteration of SDS for SANS, we have identified the formation of complex aggregates of FC_4S and SDS. The aggregation structure of the complex obtained is similar to that for pure FC_4S aggregates and is stable to the SDS concentration in the mixtures studied. Combining the contrast data sets of small angle scattering, we have obtained detailed aggregation information, including aggregation number, shape, size, and fractional ionization for the FC_4S/SDS complex aggregates. It is found that the globular-like complex aggregate, with a radius of gyration of 20 Å, consists of five FC_4S and two SDS, in an average.

1. Introduction

Recently, we have synthesized fullerene-based ionomers $C_{60}[(CH_2)_4SO_3Na]_6$ (FC_4S) and $C_{60}[CO(CH_2)_5O(CH_2)_4SO_3Na]_6$ ($FC_{10}S$) for potential biomedical applications, such as free radical scavenging or antioxidant action facilitating.[1,2] With six sulfobutyl arms randomly extending out from the C_{60} cage, the C_{60}-based star ionomers possess the desired high water solubility. Because of the constraint of the starlike morphology, both two C_{60} ionomers form aggregates of loosely arm-rich regions with a high water content in aqueous solutions, contrary to the typical micelle structure of linear surfactants, sodium dodecyl sulfoxide (SDS) for instance, having a compact hydrophobic core enclosed by a hydrophilic shell.[3]

For the bioactive C_{60} ionomers, it is crucial to know how their aggregation behavior is affected by the addition of surfactants or other amphiphilic molecules that are often used in the mimic biosystems for protein unfolding[4] or peptide aggregation preventing.[5] In our previous study, we found that $FC_{10}S$ star ionomers formed complex aggregates with SDS in water solutions.[6] In comparison with pure $FC_{10}S$ aggregates,[7] the aggregation number 18 of $FC_{10}S$ in $FC_{10}S$/SDS mixtures was significantly lower than that for pure $FC_{10}S$ aggregates by ∼50% due to the intervening of SDS molecules. The molecular ratio of SDS/$FC_{10}S$ in each aggregate was around 0.7. We also concluded that the SDS absorption efficiency to the complex should relate to the arm-rich sites (hydrophobic) of C_{60}-based star ionomers in the complex aggregates.

On the basis of the information for $FC_{10}S$/SDS aggregates obtained previously, we expect that FC_4S, with a much smaller aggregation number (∼5) and significantly shorter arms than $FC_{10}S$,[8,9] will lead to a substantially smaller association with SDS. Using a similar strategy as that for $FC_{10}S$/SDS aggregates,[6] we collect small angle neutron scattering (SANS) and small angle X-ray scattering (SAXS) data for mixtures of FC_4S and SDS. The measurement results are presented below.

2. Scattering Model and Contrast Variation

Small angle scattering (SAS) profiles for colloidal aggregates of a monodisperse size can be modeled as[10]

$$I(Q) = I_o\tilde{P}(Q)S(Q) \tag{1}$$

where $\tilde{P}(Q)$ is the normalized form factor with $\tilde{P}(0) = 1$ and $S(Q)$ is the structure factor with $S(Q) \sim 1$ at large Q values. The scattering amplitude I_o, $I(Q = 0)$, can be extrapolated from $I(Q)$ in a large Q region.[11] Here, the wave vector transfer $Q = 4\pi\sin(\theta/2)/\lambda$ is defined by the scattering angle θ and the wavelength λ of the radiation quanta. Because I_o relates to the contrast between aggregates and solvent, we can conveniently vary the contrast for different I_o values through a deuteration of the aggregation molecules or solvent or a switch of the scattering radiation quanta between X-rays and neutrons, without changing the aggregation characteristics. This contrast variation technique is useful in extracting structural information of complex aggregates, as detailed in our previous study for $FC_{10}S$/SDS mixtures.[6]

For ellipsoids of a uniform scattering length density and semimajor axis a and semiminor axis b, the form factor averaged for spatial orientation is given by[12]

$$\tilde{P}(Q) = \int_0^1 \left|\frac{3j_1(v)}{v}\right|^2 \mathrm{d}\mu \tag{2}$$

where $v = Q[a^2\mu^2 + b^2(1 - \mu^2)]^{1/2}$ and j_1 is the spherical Bessel function of the first order. For macroion solutions, the structure factor $S(Q)$ depends on the volume fraction η and the fractional

* To whom correspondence should be addressed. Fax: 886-3-5728445. E-mail: tllin@mx.nthu.edu.tw.
[†] National Tsing Hua University.
[‡] National Taiwan University.
[§] Institut für Festkörperforschung Forschungszentrum.

10.1021/jp020346r CCC: $22.00
Published on Web 11/28/2002

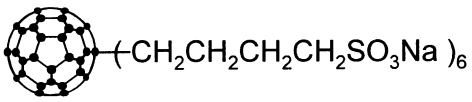

Figure 1. Scheme for the fullerene-based ionomers $C_{60}[(CH_2)_4SO_3Na]_6$ (FC_4S).

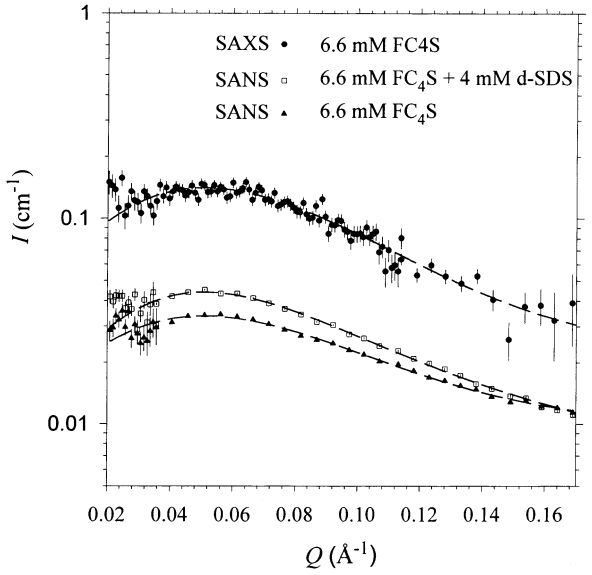

Figure 2. SANS and SAXS data for the pure FC_4S solutions in D_2O. Also shown are the SANS data for the mixture of 4 mM SDS. The dashed curves are the fitting results using an ellipsoidal model for $P(Q)$ and the MSA approximation for $S(Q)$.

ionization α of the ionic aggregates.[13] We adopt the commonly used mean spherical approximation (MSA) and the subroutine originated by Hayter et al. for $S(Q)$ in our study.[3,14] The MSA model, detailed in many articles,[3,13,14] assumes a rigid charged sphere interacting through a screened Coulomb potential. We further correct the $S(Q)$ calculated from the MSA model for a nonspherical particle effect.[13]

3. Samples and Experiment

The synthesis route for fullerene-based ionomers FC_4S (Figure 1) was reported previously.[8] D_2O solutions of 6.6 mM FC_4S mixed with 0, 4, 8, 12, 16, and 20 mM SDS were prepared for SAS. For contrast variation purpose, mixtures with 8 and 20 mM deuterated SDS (d-SDS) were also prepared. We conducted SANS measurements for the sample solutions on the 40 m SANS instrument at FRJ-2, Institute of Solid State Research (IFF), Jülich, Germany. The neutron wavelength used was 7 Å, with a wavelength spread of 18%. The sample pinhole employed was 8 mm by 8 mm, and the sample to the two-dimensional detector distance was varied from 1.4 to 8 m for covering a larger Q region. The SAXS data for the same sample solutions were collected using the 8 m SAXS instrument at the National Tsing-Hua University, Hsinchu, Taiwan.[15] All of the SAS data were corrected for sample transmission, background, and detector sensitivity and normalized to the absolute scattering scale, namely, scattering cross-section per unit sample volume $I(Q)$.[16]

4. SANS and SAXS Results

FC_4S Aggregates and FC_4S/SDS Complex. Figure 2 shows the SANS and SAXS data for the 6.6 mM FC_4S solutions in D_2O. The two sets of data are similar in profile but differ drastically in intensity. The result implies that FC_4S aggregates in water have a homogeneous structure rather than a core−shell structure like SDS micelles.[17] Using the two sets of data as a contrast constraint in a fitting algorithm (see ref 6 for details), we fit conjunctly (dotted curves) the two sets of data with the same ellipsoidal shape and the same $S(Q)$ from the MSA model. The structural parameters commonly determined by the SANS and SAXS data for the FC_4S aggregates are the dry volume of FC_4S $V_{dry} = 1696 \pm 50$ Å^3, mean aggregation number $N = 4.3 \pm 0.1$, and semiaxes $a = 36.7 \pm 2.0$ Å and $b = 17.6 \pm 1.2$ Å. The aggregation size, corresponding to a radius of gyration $R_g = 19.8$ Å ($R_g = [(a^2 + 2b^2)/5]^{1/2}$), is close to the value of 21 Å obtained from the Guinier approximation.[18] The fractional ionization α best-fitted is 0.15 ± 0.02, leading to a mean charge number of ≈4 ($6\alpha N$) for each FC_4S aggregate of $6N$ sulfobutyl arms $(CH_2)_4SO_3Na$. The fractional ionization obtained is close to that for SDS micelles of similar hydrophilic heads of SO_4Na.[19] Also, V_{dry} fitted matches the volume 1650 Å^3 estimated using 525, 27, and 80 Å^3 for the dry volumes of C_{60}, CH_2, and SO_3Na, respectively.[3] The hydration number 1340 of the aggregate, deduced from the volumes of water (30.3 Å^3), FC_4S, and the aggregate, indicates a high water volume content of 85% in the watery FC_4S aggregates.

Using the same ellipsoidal model with the MSA model, we can fit the data for the mixture of 4 mM SDS seamlessly (Figure 2). In the fitting process, we have assumed no scattering contribution from SDS micelles, since the SDS concentration is substantially lower than the critical micelle concentration (CMC; 8 mM) of SDS.[20] Also, we have adopted a dry volume of SDS, 405 Å^3, reported by Sheu et al. for reducing free parameters.[21,22] The structural information suggested by the fitting result includes 4.5 and 1.8, respectively, for the aggregation numbers of FC_4S and SDS in each aggregate, the semiaxes $a = 39.6$ Å and $b = 15.5$ Å, and the fractional ionization 0.14 for the complex aggregates. Except for the small absorption of SDS into FC_4S aggregates, these structural parameters fitted are nearly the same as those for pure FC_4S aggregates. From the aggregation numbers obtained, we deduce that about 2.6 mM SDS adsorbs to FC_4S aggregates, whereas the rest of 1.4 mM SDS remains as free monomers in the mixture of 4 mM SDS.

Pure SDS Micelles Coexisting with FC_4S/SDS Aggregates. The aggregation behavior for FC_4S/SDS mixtures with SDS concentrations close or larger than the CMC of SDS is more complicated due to a possible coexistence of pure SDS micelles in the system. Fortunately, the scattering contribution from pure SDS micelles is insignificant for SAXS, since the SAXS intensity from FC_4S/SDS mixtures is constantly dominated by the high scattering contrast of C_{60} (charge density $\rho \approx 0.69$ e$^-$/Å^3) of FC_4S and is insensitive to SDS monomers ($\rho \approx 0.39$ e$^-$/Å^3) or micelles in water ($\rho \approx 0.37$ e$^-$/Å^3). Therefore, we can monitor conveniently the structural change of FC_4S aggregates in the mixtures upon the change of SDS concentration using SAXS. In fact, the series of SAXS profiles observed for the mixtures of 6.6 mM FC_4S with 0, 8, 12, 16, and 20 mM SDS is very much the same (selected data are shown in Figure 3). The SAXS result implies that the FC_4S aggregation behavior essentially does not change with the SDS concentration in the mixtures.

On the other hand, because neutrons are much more sensitive to SDS micelles (in D_2O, scattering length density contrast $\Delta\rho \approx 6.0 \times 10^{-6}$ Å^{-2}) than FC_4S aggregates ($\Delta\rho \approx 3.0 \times 10^{-6}$ Å^{-2}), we can use SANS to monitor the SDS aggregation behavior in the mixtures. The SANS profiles (Guinier plot presentation in Figure 4) measured for the same series of sample

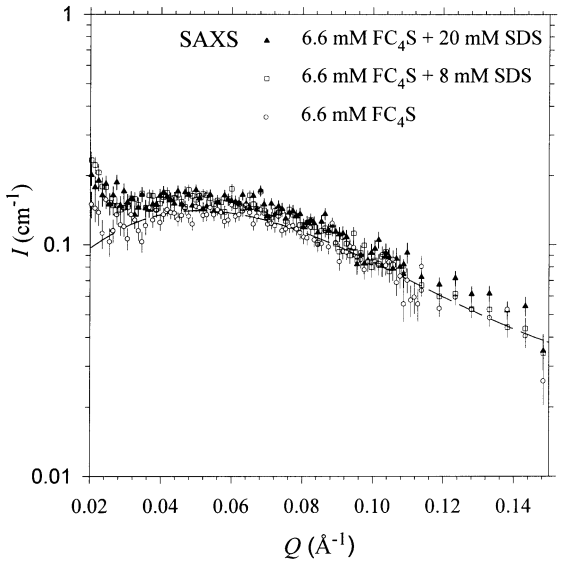

Figure 3. Typical SAXS data for the 6.6 mM FC_4S mixtures with different SDS concentrations (only 8 and 20 mM SDS data sets are shown). The data and the fitting curve for the pure FC_4S solution are also shown for a comparison.

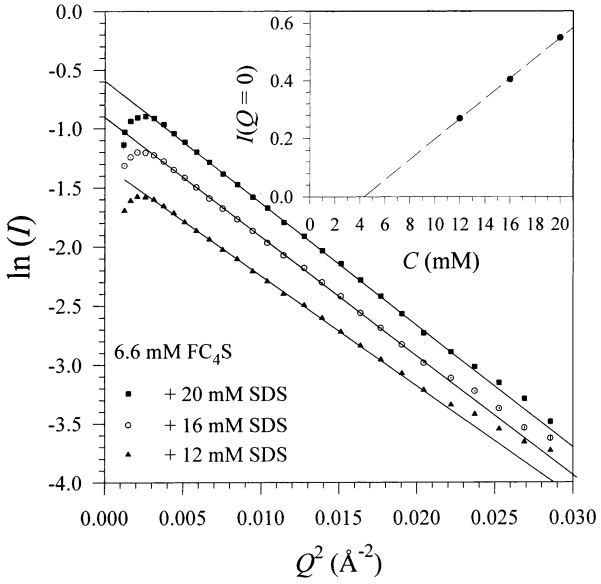

Figure 4. Guinier plot presentation for the SANS data of FC_4S/SDS mixtures. The solid lines are the corresponding Guinier approximations for the data sets. The inset shows a linear relationship (dashed line) of the extrapolated I_o with the SDS concentration.

mixtures exhibit a linear increase in the scattering intensity, when the SDS concentration increases from 12 to 20 mM SDS. This indicates that the scattering profile and intensity of the mixture are, indeed, well-dominated by the shape and number density of SDS micelles after 12 mM SDS. Whereas the SDS concentration is smaller than 8 mM, the scattering concentration of SDS micelles is comparable to that for FC_4S (see below).

Using the Guinier approximation (solid lines in Figure 4),[18] we extrapolate I_o ($Q = 0$) for the SANS profiles (Figure 4) of the mixtures with 12, 16, and 20 mM SDS. As shown in the inset of Figure 4, these I_o values fall well in a linear relationship (dotted line) with the SDS concentration, C. An effective CMC, $C_o = 4.3 \pm 0.3$ mM, for the threshold concentration of the formation of SDS micelles in the FC_4S/SDS mixtures, can be extracted sharply from the intercept at $I_o = 0$. In addition, the slope of the dotted line fitted represents a mean concentration-normalized I_o value, $I_o/C = N\Delta\rho^2$,[13] where we can also deduce a common aggregation number N_{SDS} of 100 ± 5 for the pure SDS micelles in these three mixtures. The averaged radius $R_{SDS} = 22.0 \pm 0.8$ Å for the SDS micelles is extracted from the slopes of the solid lines for the Guinier approximation (see Figure 4). Here, we have neglected the relatively small contribution of the FC_4S/SDS aggregates and approximated the SDS micelles with a spherical model of a homogeneous structure, which is reasonable as shown by Sheu et al.[19] With the effective CMC value of SDS taken into account, we now can calculate the number density of SDS micelles in the mixtures using $n_{SDS} = (C - C_o)/N_{SDS}$.

The observed CMC for SDS in the mixing system can be attributed partly to the SDS adsorbed into the complex aggregates and partly to the free SDS monomers. Because of the amount of SDS adsorbed to the complex aggregates, $C_{ads} \approx 2.6$ mM is essentially the same for mixtures of 6.6 mM FC_4S (see Table 1), and the free SDS monomers concentration ($= C_o - C_{ads}$) saturates at 1.7 mM as the SDS concentration in the mixture grows larger than C_o where the formation of SDS micelles launches.

The aggregation characteristics for the SDS micelles in the mixtures obtained above are quite useful in selecting the initial values for fitting parameters in our fitting algorithm that takes into account the scattering contributions of FC_4S/SDS complex and pure SDS micelles in the same time. Using the same model mentioned previously, we fit the contrast data sets of 8 and 20 mM cases, respectively. In each case, we fit conjunctly the three contrast data sets, including the SANS with SDS, SANS with d-SDS, and SAXS with SDS. Note that because the number density of SDS micelles is much smaller than that for FC_4S/SDS complex aggregates in all the mixtures studied, we neglect the partial structure factor[13] of SDS micelles in the model fitting. Namely, the structure factor of the mixing system is approximated by the $S(Q)$ calculated from the MSA model with the volume fraction and the fractional ionization contributed solely by the complex aggregates FC_4S/SDS. The highly consistent fitting results shown in Figures 5 (8 mM case) and 6 (20 mM case) support strongly our picture on the FC_4S/SDS aggregates, which have a stable aggregation structure under the addition of SDS. The structural parameters obtained from the fitting are summarized in Table 1.

We have also conducted SANS and SAXS measurements for sample mixtures of a FC_4S concentration (13.2 mM) two times higher than the previous one and a SDS (d-SDS) concentration of 17.3 mM. The SAS result reflects generally the same aggregation characteristics as those for the previous system of 6.6 mM FC_4S. We will detail the results in a later paper.

5. Conclusions and Discussion

Using SAXS and SANS with the contrast variation method, we have found that C_{60}-based star ionomers FC_4S associate weakly with SDS in aqueous mixtures (1:0.2 molecular ratio in the complex aggregate), as compared to the $FC_{10}S$/SDS complex aggregates (1:0.7). As a consequence, the FC_4S aggregation structure (shape, size, and aggregation number) is relatively stable upon the addition of SDS surfactants in the mixtures. The lower SDS absorption efficiency for FC_4S aggregates can be realized from the significantly smaller aggregation number and shorter sufbotyl arms than that for $FC_{10}S$ aggregates, as we have mentioned in the beginning. Structurally speaking, the starlike morphology prevents FC_4S from a compact aggregation. As a consequence, the loose hydrophobic regions formed in the FC_4S aggregates with a high

TABLE 1: Structural Parameters Fitted for Pure FC_4S Aggregates and the Mixed FC_4S/SDS Aggregates in the Mixtures of 6.6 mM FC_4S with 4 mM SDS, 8 mM SDS (or d-SDS), and 20 mM SDS (or d-SDS)[a]

		6.6 mM FC_4S (SANS, SAXS)	+4 mM SDS (SANS)	+8 mM SDS (d-SDS) (SANS, SAXS)	+20 mM SDS (d-SDS) (SANS, SAXS)
mixed aggregate	N	4.3 ± 0.1	4.5	4.5[b]	4.5[b]
	N_s	0	1.9	1.9	1.9[b]
	a (Å)	36.9 ± 1.9	41	39.6[b]	39.6[b]
	b (Å)	17.6 ± 1.2	15.2	15.5[b]	15.5[b]
	α	0.15 ± 0.02	0.14	0.072	0.090
	V_{dry} (Å^3)	1695 ± 50	1697	1625	1563
pure SDS micelles	N_{SDS}	0	0	76	100
	R_{SDS} (Å)	22[b]	22[b]	22[b]	24

[a] Parameters listed are common for the contrast SANS and SAXS data sets. The smearing effect of $I(Q)$ due to the beam divergence and the wavelength dispersion of the beam were taken into account for the SANS and SAXS data, respectively.[6] Note that fitting parameters for the complex aggregates are less sensitive at higher SDS concentrations due to the increasing larger contribution from SDS micelles. Fitting parameters obtained for the SANS data of the mixtures with 12 and 16 mM SDS are nearly the same as that for the mixture of 20 mM SDS. [b] Fix parameters. N and N_s, aggregation numbers for FC_4S and SDS in ellipsoidal FC_4S or FC_4S/SDS aggregates; a and b, semimajor and semiminor axes for the ellipsoidal aggregates; α, fractional ionization for the aggregates; V_{dry}, dry volume for FC_4S; N_{SDS} and R_{SDS}, aggregation number and radius for the pure SDS micelles coexisting with FC_4S/SDS aggregates in the mixtures.

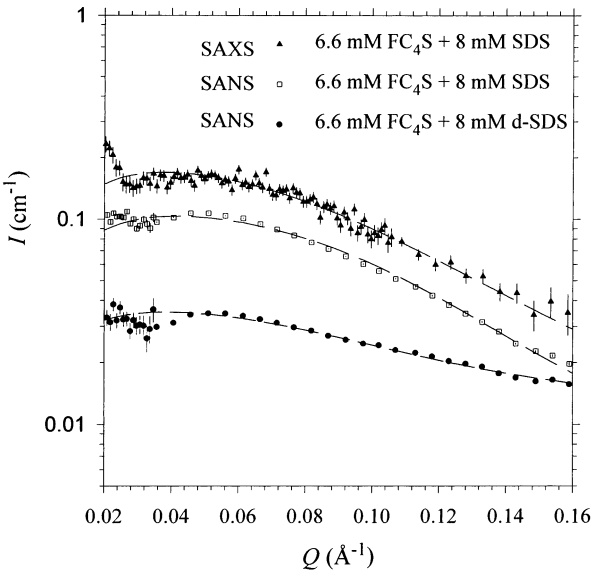

Figure 5. SAS data sets for the mixtures of 6.6 mM FC_4S with 8 mM SDS case. The data are fitted (dashed curves) using the same model as described previously.

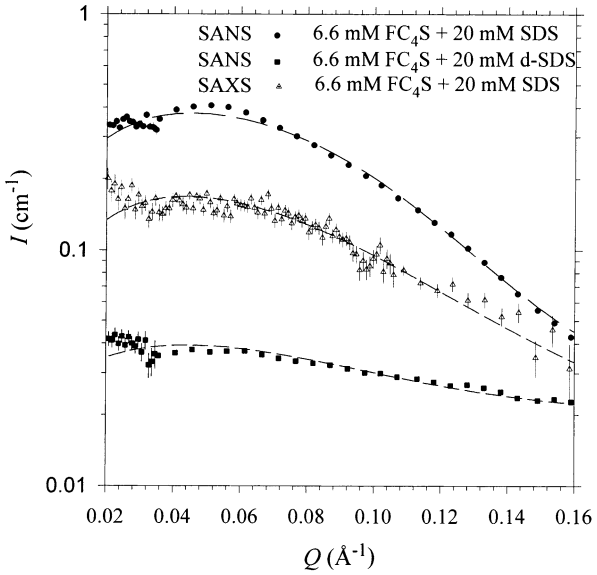

Figure 6. SAS data sets for the mixtures of 6.6 mM FC_4S with 20 mM SDS case. The data are fitted (dashed curves) using the same model as described previously. The slighter larger discrepancy between the fitting curve and the SANS data for the mixture of 20 mM SDS may result from the neglect of the partial structure factor of SDS micelles in the fitting algorithm.[13]

water content may only provide small attractions to SDS and saturate with a small amount of SDS quickly. This low association with SDS found for FC_4S aggregates may have certain advantages in systems where SDS is used for protein unfolding[4] or peptide aggregation-preventing agents.[5] For instance, the activity of the bioactive C_{60}-based star ionomers with proteins or peptides may be less interfered by the protein denaturing agent, SDS, added into the systems.

On the other hand, the lower CMC value for SDS found in the FC_4S/SDS system may not be surprising. The counterions Na^+ released from the ionization of FC_4S aggregates can influence the aggregation behavior of SDS micelles and increase appreciably the aggregation number of SDS micelles, as reported by Sheu et al.[3] This can be understood from a stronger screening effect due to the higher Na^+ concentration, which helps in reducing the charge interactions of SO_3^- groups on the surface of SDS micelles, therefore, reducing the formation energy of SDS micelles.

For a comparison, the lowered CMC for SDS in the FC_4S/SDS mixing system observed is 4.3 mM, under the influence of the 4 mM Na^+ released from 6.6 mM FC_4S ($\alpha = 0.1$ approximated). These values agree well with those from the surface pressure−area isotherm measurement using a Langmuir trough[23] and the microcalorimetry result[24] for the Na^+ effect to the CMC value of SDS in pure SDS systems. Furthermore, we have also observed a very similar CMC reducing effect for SDS in the sister system of $FC_{10}S$/SDS.[25]

Acknowledgment. We acknowledge the support of FRJ-2 for the SANS beam time. This work was supported by the grant for the user-training program of TRR2 project of the Institute of Nuclear Energy Research and the National Science Council, Grant NSC89-2113-M-007-060.

References and Notes

(1) Lai, Y. L.; Chiou, W.-Y.; Lu, F. J.; Chiang, L. Y. *Br. J. Pharmacol.* **1999**, *126*, 778.
(2) Huang, S. S.; Chen, Y. H.; Chiang, L. Y.; Tsai, M. C. *Fullerene Sci. Technol.* **1999**, *7* (4), 551.
(3) Sheu, E. Y.; Wu, C.-F.; Chen, S.-H. *J. Phys. Chem.* **1986**, *90*, 4179.
(4) Chen, S.-H.; Teixeira, J. *Phys. Rev. Lett.* **1986**, *57*, 2583.
(5) Marcinowski, K. J.; Shao, H.; Clancy, E. L.; Zagorski, M. G. *J. Am. Chem. Soc.* **1998**, *120*, 11082.

(6) Jeng, U.; Lin, T.-L.; Liu, W.-J.; Tsao, C.-S.; Canteenwala, T.; Chiang, L. Y.; Sung, L. P.; Han, C. C. *Physica A* **2002**, *304*, 191.
(7) Liu, W.-J.; Jeng, U.; Lin, T.-L.; Canteenwala, T.; Chiang, L. Y. *Fullerenes Sci. Technol.* **2001**, *9*, 131.
(8) Jeng, U.; Lin, T.-L.; Tsao, C.-S.; Lee, C.-H.; Wang, L. Y.; Chiang, L. Y.; Han, C. C. *J. Phys. Chem. B* **1999**, *103*, 1059.
(9) Tsao, C.-S.; Lin, T.-L.; Jeng, U. *J. Phys. Chem. Solid*s **1999**, *60*, 1351.
(10) Lin, T.-L. *Physica B* **1992**, *180*−*181*, 505.
(11) Chen, S. H. *Annu. Rev. Phys. Chem.* **1986**, *37*, 351.
(12) Feigin, L. A.; Svergun, D. I. *Structure Analysis by Small-Angle X-ray and Neutron Scattering*; Plenum: New York, 1987; p 69.
(13) Chen, S. H.; Lin, T. L. *Methods of Experimental Physics*−*Neutron Scattering in Condensed Matter Research*; Sköd, K., Price, D. L., Eds.; Academic Press: New York, 1987; Vol. 23B, Chapter 16.
(14) Hayter, J.; Penfold, J. *Mol. Phys.* **1981**, *42*, 109.
(15) Linliu, K.; Chen, S.-A.; Yu, T. L.; Lin, T.-L.; Lee, C.-H.; Kai, J.-J.; Chang, S.-L.; Lin, J. S. *J. Polym. Res.* **1995**, *2*, 63.
(16) Glinka, C. J.; Barker, J. G.; Hammouda, B.; Krueger, S.; Moyer, J. J.; Orts, W. J. *J. Appl. Crystallogr.* **1998**, *31*, 430.
(17) Zemb, T.; Charpin, P. *J. Phys.* **1985**, *46*, 249.
(18) Guinier, A.; Fournet, G. *Small-Angle Scattering of X-rays*; John Wiley and Sons: New York, 1955.
(19) Sheu, E. Y.; Wu, C.-F.; Chen, S.-H. *Phys. Rev. A* **1885**, *32*, 3807.
(20) Cabane, B.; Duplessix, R. *J. Phys.* **1982**, *43*, 1529.
(21) Sheu, E. Y.; Chen, S.-H. *J. Phys. Chem.* **1988**, *92*, 4466.
(22) Cabane, B.; Duplessix, R.; Zemb, T. *J. Phys.* **1985**, *46*, 2161.
(23) Private communication.
(24) Chatterjee, A.; Moulik, S. P.; Sanyal, S. K.; Mishra, B. K.; Puri, P. M. *J. Phys. Chem. B* **2001**, *105*, 12823.
(25) Data not published.